

# Investigation of a hyperbranched polyurethane as a solid-state phase change material

Li Liao · Qi Cao · Hongqing Liao

Received: 30 October 2009 / Accepted: 7 January 2010 / Published online: 16 January 2010  
© Springer Science+Business Media, LLC 2010

**Abstract** As phase change material (PCM), doped hyperbranched polyurethane (D-HBPU) was synthesized by PEG6000 via two steps: at first take tetrafunctional pentaerythritol as soft segment, and then use liquefaction-modified isocyanate, and chain extender as hard segment. This material's molecular structure, phase change behaviors, thermal-resistant property, and crystalline morphology had been investigated by Fourier transform infrared spectroscopy, differential scanning calorimetry, thermogravimetric analyses, wide-angle X-ray diffraction (WAXD), and polarization optical microscopy (POM). Results showed that D-HBPU was a typical solid-state PCM with better heat storage property and thermal resistance when compared with hyperbranched polyurethane. The transition enthalpy and the main decomposition temperature of D-HBPU were 125.0 J/g and 437 °C, respectively. From WAXD and POM, the results suggested that D-HBPU has good crystallization.

## Introduction

Phase change materials (PCMs) have attracted lots of researcher's interest recently because of their high storage density and constant temperature during phase change processes. Their applied field is extensive, such as solar energy

storing, smart air-conditioning buildings, agricultural greenhouse, temperature-regulating textiles, heat management of electronics, telecommunications and microprocessor equipment, biomedical and biological-carrying systems and so on [1–7]. In recent years, energy crisis is becoming more and more serious, so a great number of organic, inorganic, polymeric, and eutectic compounds have been studied [8] for entreating it. According to their phase change stated, PCMs can be ranged three groups: solid–solid PCMs, solid–liquid PCMs, and liquid–gas PCMs [9]. Solid–solid PCMs include inorganic solid–solid PCMs, organic solid–solid PCMs, and polymer-based solid–solid PCMs. Among all these materials, polymer-based solid–solid PCMs have developed rapidly because they have been found to exhibit many obvious advantages: no liquid or gas generation, small volume change, and no seal needed [10], easily being processed into arbitrary shape, even being used as a system material directly. Unfortunately, few of the solid–solid PCMs have been reported in the past. Ascribed to the excellent integrated performance, composite polymeric solid–solid PCMs are focused on the academia and industrial field [11, 12].

Over the last two decades, many researchers are concentrating on the highly branched three-dimensional molecular polymeric materials like hyperbranched polymers for different advanced applications because of their unusual and unique characteristics. The research of branching into polymers has been used extensively to modify the structure of synthesized materials. In the field of PCMs, polyurethane with hyperbranched polyester as chain extender has been reported. Cao and Liu [13] prepared hyperbranched polyurethane for thermal energy storage as a novel solid–solid PCM. The phase transition enthalpy was more than 100 J/g with a transition point at 67 °C.

---

L. Liao · Q. Cao (✉) · H. Liao  
Key Laboratory of Environmentally Friendly Chemistry  
and Applications of Ministry of Education, Xiangtan University,  
411105 Xiangtan, Hunan Province, People's Republic of China  
e-mail: wjcaoqi@163.com

L. Liao  
e-mail: liao736@163.com

In order to improve the thermal properties including phase change enthalpy and thermal resistance of hyperbranched polyurethane (HBPU) further, the material could be doped with other PCMs. In this article, as PCMs, doped hyperbranched polyurethane (D-HBPU) had been synthesized by PEG6000 via two steps: at first take tetrafunctional pentaerythritol as soft segment, and then use liquefaction-modified isocyanate, and chain extender as hard segment. The material's molecular structure, phase change behaviors, thermal-resistant property, and crystalline morphology were investigated by Fourier transform infrared spectroscopy (FT-IR), differential scanning calorimetry (DSC), thermogravimetric analyses (TGA), wide-angle X-ray diffraction (WAXD), and polarization optical microscopy (POM). The results were discussed herein. This novel high-performance solid-state phase change heat storage material maybe has extensive potential applications.

## Experimental

### Materials

Polyethylene glycol (PEG,  $M_n = 6000$ , from Shantou Guanghua Chemical Reagent Co. Inc., China) was degassed and dried in a round flask under high vacuum (20 Pa) at 100–120 °C for 3–4 h.

Pentaerythritol (PE, from Guangzhou Chemical Regents Co., China) was used with further purification to remove trace water.

Liquefaction modified 4,4'-diphenylmethane diisocyanate (L-MDI, with 23 wt% isocyanates) was obtained by the liquefactions of MDI in the presence of little molecular glycol-dominant reaction reagents in our laboratory [14].

Boltorn<sup>®</sup> H20 (second generation,  $M_w = 1750$  g/mol, hydroxyl number equals 470–500 mg KOH/g, from Perstorp Specialty Chemicals, Sweden) was dried at 60 °C under vacuum prior to use.

*N,N*-Dimethylformamide (DMF, from Shantou Guanghua Chemical Reagent Co. Inc., China) was dried by 5-Å molecular sieve for 24 h followed by distillation before use.

### Synthesis of doped hyperbranched polyurethane

A three-neck round-bottom flask was equipped with nitrogen gas inlet, mechanical stirrer, and thermometer, for this polymerization reaction. The general synthesis procedure of doped hyperbranched polyurethane with 90-wt% soft segment content (SSC) as follows: dehydrated PEG6000 9.95 g with a little pentaerythritol 0.05 g and excess of L-MDI 1.0275 g in freshly distilled DMF were mixed with stirring in a thermostatic oil-bath at 80 °C for

5 h. A predetermined of Boltorn<sup>®</sup> H20 (0.0837 g) was dissolved in dried DMF and added to the mixture (molar ratio:  $-\text{NCO}/-\text{OH} = 1$ ). After stirring for another 2 h, the reaction mixture was cast in a glass pan. Heating at 80 °C in a vacuum oven for 24 h, after which the polymer films were obtained. The samples were kept in vacuum at room temperature for 2 weeks before testing.

Hyperbranched polyurethane with 90-wt% SSC has the same process of synthesis.

### Characterization

#### *Infrared spectroscopy*

In order to identify the chemical structure of the samples, FT-IR spectra were recorded in the range of 400–4000  $\text{cm}^{-1}$  on a FT-IR170 (PE Company) spectrometer. The KBr-pressed disk technique was used.

#### *Differential scanning calorimetry*

The DSC test was performed on a PE Q10 DSC instrument. About 5 mg of the sample was placed in sealed aluminum pan and heated to 120 °C at a heating rate of 10 °C  $\text{min}^{-1}$ , kept at this temperature for 3 min and then cooled to  $-20$  °C at a cooling rate of 10 °C  $\text{min}^{-1}$ . Second heating scanning curves from  $-20$  to 120 °C were recorded. Latent heat of fusion was calculated using the area under the peak and melting temperature was estimated by the tangent at the point of greatest slope on the face portion of the peak [15].

#### *Thermogravimetric analyses*

TGA were carried out using TA Instruments Co. thermal analysis system (SHIMADZA TG-40, Japan). About 10 mg of the dried sample was weighed into an alumina crucible and the profiles were recorded from room temperature to 600 °C at a heating rate of 10 °C  $\text{min}^{-1}$ .

#### *Wide-angle X-ray diffraction*

WAXD was carried out with a Rigaku D/Max-1200 X-ray diffractometer. The incident X-ray was  $\text{CuK}\alpha$  with a power of 40 kV, 25 mA, passed through a nickel filter. Bragg's angle  $2\theta$  is set from ca. 5° to 40°.

#### *Polarization optical microscopy*

An observation of POM was performed on a Leitz Laborlux 12POL microscope equipped with a video camera. The sample was placed between a microscope glass and a cover slip, and heat with a Leitz 350 hot stage.

## Results and discussions

### Visual observation

Phase transition behavior of samples is an important property to facilitate production, handling, and application. In the whole phase change process, solid D-HBPU is hard and slightly yellow in color at room temperature. When the temperature rises to 60 °C, the polyurethane becomes transparent. It is quite transparent as the temperature increases. After up to 100 °C, the D-HBPU remains solid. The visual observation indicates that PEG and PE in the D-HBPU in solid state even when the temperature rises to 100 °C, over 41 °C above the melting point of D-HBPU. As we know, pristine PEG is typical solid–liquid PCM [16], and PE is polyalcohol solid–solid PCM [17], but in D-HBPU, both of them present solid-state phase transition behavior. Because the hard segment domains, serving as skeleton, restrict the free movement of soft segment [18], when it is heated to the temperature 30–50 °C above the material's melting point, PEG and PE in D-HBPU were still observable in solid state. No liquid leaked from the sample.

### FT-IR spectra evaluations

FT-IR spectra of the materials and synthesized foams are presented in Figs. 1 and 2, respectively. D-HBPU and HBPU have similar absorption band. From Fig. 2, the band of –OH stretching vibration at 3425  $\text{cm}^{-1}$  is associated with the free  $\text{H}_2\text{O}$ , –OH groups of non-bonded polyol, or –OH groups within the polymer structure. Compared with Fig. 1, the strong hydroxyl absorption peak becomes weak

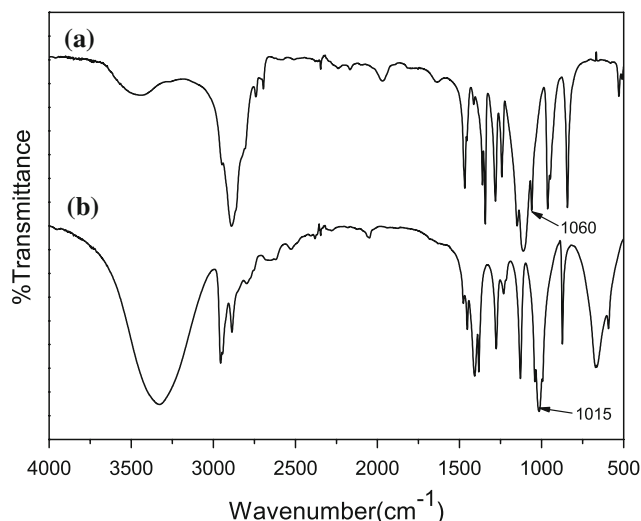


**Fig. 1** The FT-IR spectra of materials: (a) PEG6000 and (b) PE

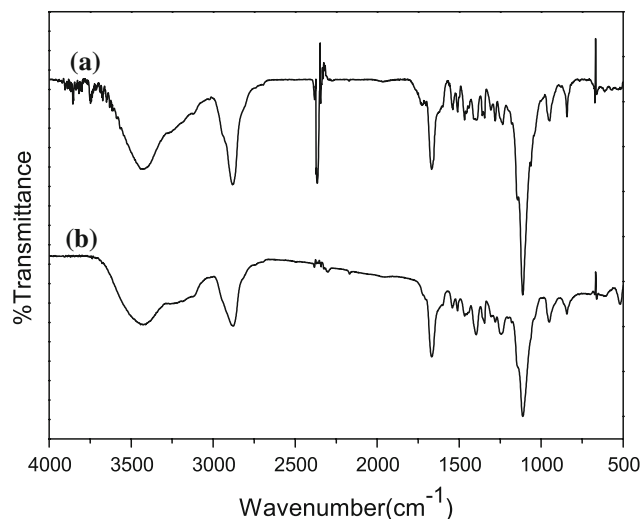


**Fig. 2** The FT-IR spectra of samples: (a) HBPU and (b) D-HBPU

and wide, especially PE, and the characteristic absorption of primary hydroxyl at 1060  $\text{cm}^{-1}$  (PEG) and 1015  $\text{cm}^{-1}$  (PE) disappeared. These results imply that PEG and PE have been reacted. The transmission band of – $\text{CH}_2$  and – $\text{CH}$  appeared at 2877  $\text{cm}^{-1}$ . As marked in the curves (Fig. 2), amide bond I (1668  $\text{cm}^{-1}$ ), amide bond II (1510  $\text{cm}^{-1}$ ), and vibration peak of conjugated double bonds of benzene ring (1541  $\text{cm}^{-1}$ ) were found distinctly. And peaks related to the new formed ester group (– $\text{C}=\text{O}$ ) at 1730  $\text{cm}^{-1}$  observed in the spectrum. FT-IR analysis results confirm that high molecular weight doped hyper-branched polyurethane had been gained through the chemical reaction of PEG, PE, L-MDI, and Boltorn<sup>®</sup> H20.

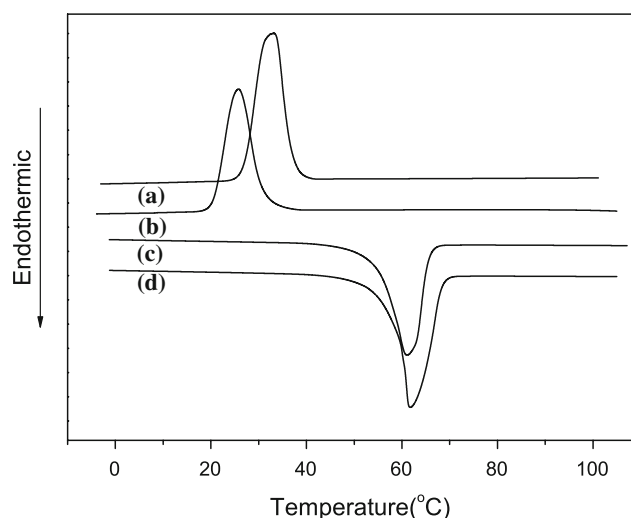


**Fig. 3** DSC curves of samples: (a) cooling curve of D-HBPU, (b) cooling curve of HBPU, (c) heating curve of HBPU, (d) heating curve of D-HBPU

**Table 1** Thermal property of HBPU and D-HBPU measured by DSC analysis

Samples	Phase transition	Transition temperature $T_i$ (°C)		Enthalpy of phase transition $\Delta H$ (J/g)	
		Heating cycle	Cooling cycle	Heating cycle	Cooling cycle
HBPU	Solid–solid	55.7	30.8	115.7	112.4
D-HBPU	Solid–solid	59.0	36.8	125.0	120.6

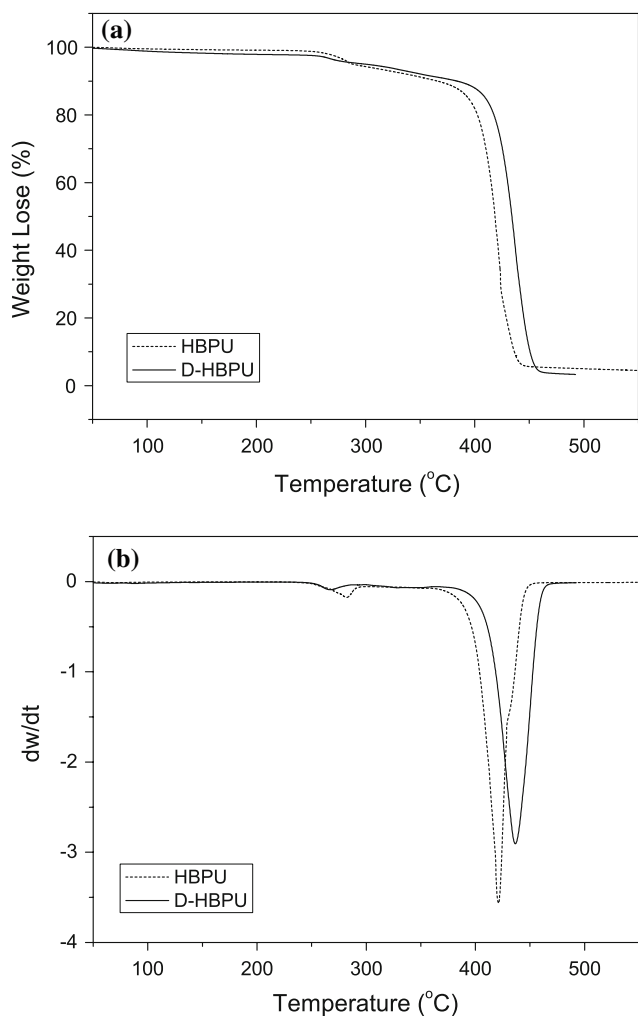
Thermal properties investigations

Figure 3 displays the DSC curves of hyperbranched polyurethane and doped hyperbranched polyurethane. The data of the corresponding phase transition temperature and enthalpy are summarized in Table 1. It can be seen that the thermal characteristics of D-HBPU are very close to those of HBPU. This is because there is no chemical reaction between PEG and PE in the preparation of the doped PCM. The DSC measurement of D-HBPU with 90-wt% SSC shows heat absorption at about 59.0 °C in the heating cycle, suggesting that a phase transition has taken place.

Both HBPU and D-HBPU undergo phase transition with high transition enthalpy, the transition enthalpy of HBPU and D-HBPU is 115.7 and 125.0 J/g, respectively. For the D-HBPU, the fusion enthalpy is higher in comparison with HBPU, which meant that the endothermic and exothermic capacity of D-HBPU strengthened. This is attributed to the structure of pristine PE. PE is a tetra-hydroxyl compound with high crystallization and large enthalpy (289 J/g) [19]. It reacted with L-MDI and formed part of soft segment, could make some contributions to the heat storage like PEG. Because of suitable phase change temperature, D-HBPU can be used to store thermal energy in the lower temperature fields, such as phase change floor or solar storage, and the large enthalpy of D-HBPU enable it plays a very prominent role in many other fields.

Thermogravimetric analysis

TGA is frequently used to assess the thermal-resistant property of PCMs. This property is important because processes to manufacture various PCM products are subject to high temperature. The TGA and DTG curves of D-HBPU are shown in Fig. 4. It was obviously observed that the degradation of two samples was mainly consisted of two stages under the protection of nitrogen; D-HBPU has better heat-resistant performance. The first decomposition



**Fig. 4** TGA (a) and DTG (b) curves of HBPU and D-HBPU

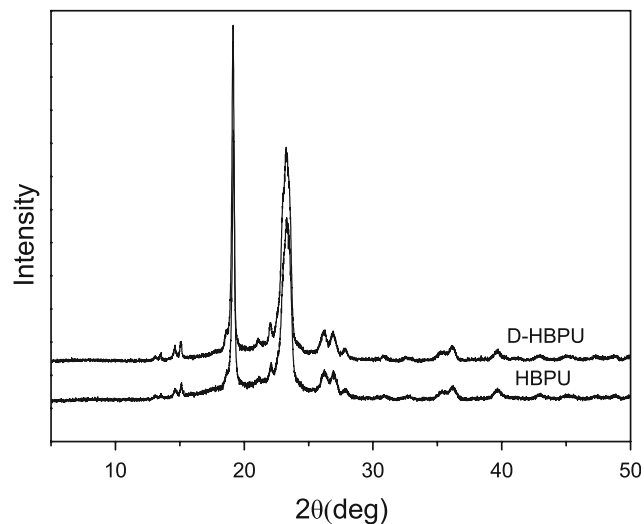


**Fig. 5** WAXD patterns of HBPU and D-HBPU

temperatures of HBPU and D-HBPU were 283 and 267 °C, respectively. In this step, the mass loss is little. In the second step, the onset temperature and distinct decomposition peak point of HBPU were 389 and 421 °C, while those of D-HBPU were 403 and 437 °C when compared D-HBPU with HBPU, the initial decomposition temperature and peak point of decomposition increased about 14 and 16 °C, this can be explained by the addition of PE, the steric structure of PE induced cross-linking lightly in the polymer, and the degree of rigidity increased. Besides, hydrogen bonds

among molecules in D-HBPU strengthened, because more –OH were brought in the system, they connect with each other. Thus, the thermal resistance was elevated after doping PE. These results suggest that D-HBPU with good heat-resistant performance will have a broad applicable temperature range.

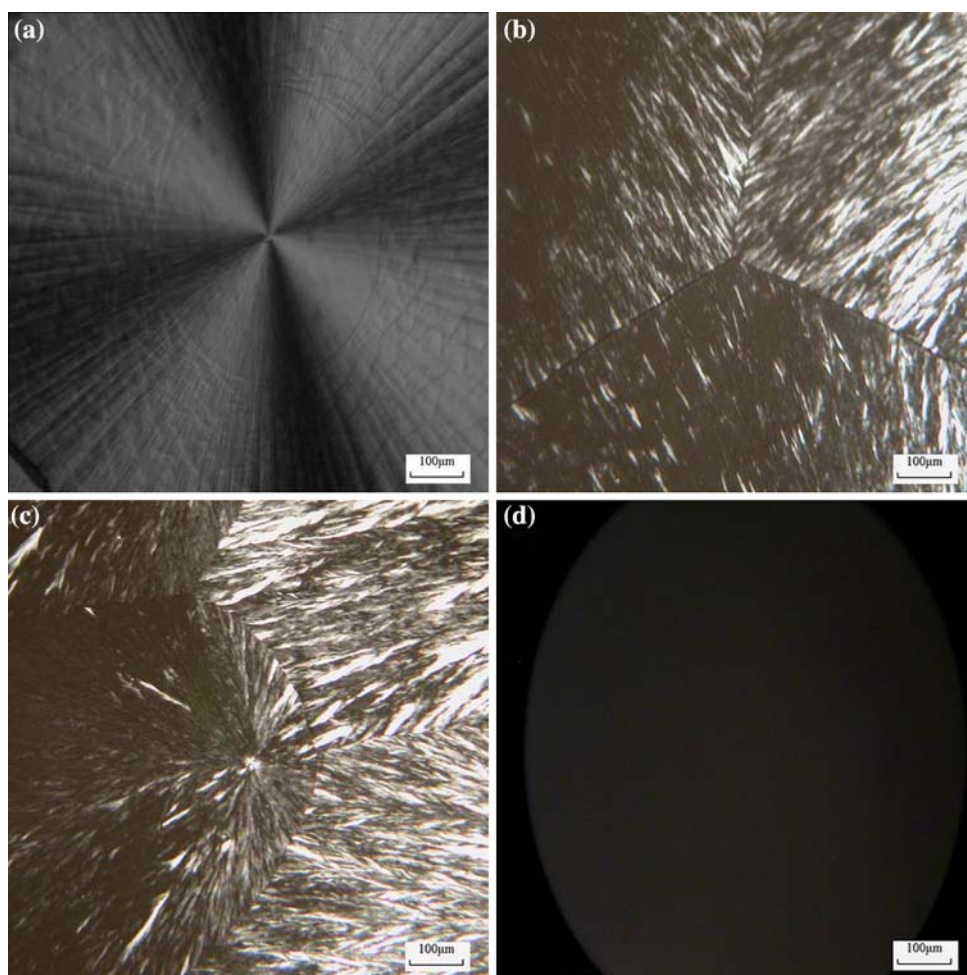
#### Crystallization morphology investigation

To reveal the crystallization morphology, WAXD technique was used to investigate the phase change behavior of the materials. Figure 5 shows the WAXD patterns of two samples, and the relational data were shown in Table 2. Through WAXD patterns and data, it is easily observed that HBPU and D-HBPU had similar diffraction patterns on which diffraction angle and crystal plane distance are nearly the same. HBPU showed two main diffraction peaks at 19.15° and 23.29°, and the peaks of D-HBPU appeared at 19.12° and 23.25°, which indicated that they had the same crystal structure and unit cell type, namely, the crystal structure of PEG in D-HBPU unchanged after doping PE. From Table 2, the difference between them was

**Table 2** Highest three peaks of WAXD of HBPU and D-HBPU

Samples	Peaks	$2\theta$ (°)	$d$ (nm)	Intensity	Half-width	Rel intens (%)
HBPU	1	19.15	4.630	2871	0.194	100.0
	2	23.28	3.816	1877	0.768	65.4
	3	36.19	2.480	269	–	9.4
D-HBPU	1	19.15	4.639	3566	0.183	100.0
	2	23.25	3.823	2173	0.767	60.9
	3	36.12	2.485	232	–	6.5

**Fig. 6** POM micrographs of samples: **a** PEG6000 at room temperature, **b** HBPU at room temperature, **c** D-HBPU at room temperature, **d** D-HBPU at 80 °C





that the diffraction peak height and half-width, those of D-HBPU were higher and narrower than HBPU, it demonstrates that the dimension of crystallite becomes larger and the degree of crystallization increased after doping. So the enthalpy of D-HBPU exceed HBPU a little, these results are in good agreement with the DSC results discussed above.

The POM micrographs can be used for investigating the morphology too. Some micrographs about branched morphology have been presented in other literature [20]. Figure 6 displays POM micrographs of pure PEG6000, HBPU, and D-HBPU at 200 magnifications. In Fig. 6, the micrographs show obvious cross-extinction patterns, it can be seen that all of them are crystalline and have crystal spherulites at room temperature. However, the spherulites size of HBPU and D-HBPU are smaller than that of PEG6000 due to the restriction of hard segment [18]. During the transition process, the spherulite of D-HBPU has no change with the temperature increasing before the transition point, when the temperature approached melting point, the spherulites starts to be destroyed and completely disappeared finally. The visual field of POM is dark, but no liquid is observed in this process, which proved that the material is solid–solid state in the temperature range of phase change.

## Conclusions

In this study, the D-HBPU was prepared via doping PE. From the above analysis, D-HBPU is efficient thermal energy storage material with high enthalpy and suitable transition temperature, and it shows typical solid–solid phase change property, furthermore, its thermal resistance is better than HBPU because of the addition of PE, which formed partly cross-linking and increased material's

rigidity. According to the characters of this material, it can be concluded that D-HBPU is promising in application as a shape-stabilized solid–solid PCM, and it has great potential advantages for thermal energy storage.

## References

- Gschwander S, Schossig P, Henning HM (2005) *Sol Energy Mater Sol Cells* 89:307
- Farid MM, Khudhair AM, Razack SAK, Al-Hallaj S (2004) *Energy Convers Manag* 45:1597
- Fang XM, Zhang ZG (2006) *Energy Build* 38:377
- Zhang YP, Zhou GB, Lin KP, Zhang QL, Di HF (2007) *Build Environ* 42:2197
- Pandian R, Kooi BJ, De Hosson JTM, Pauza A (2007) *J Appl Phys* 101:053529
- Mondal S (2008) *Appl Therm Eng* 28:1536
- Sharma A, Tyagi VV, Chen CR, Buddhi D (2009) *Renew Sustain Energy Rev* 13:318
- Kenisarin M, Mahkamov K (2007) *Renew Sustain Energy Rev* 11:1913
- Meng QH, Hu JL (2008) *Sol Energy Mater Sol Cells* 92:1260
- Xi P, Gu XH, Cheng BW, Wang YF (2009) *Energy Convers Manag* 50:1522
- Su JC, Liu PS (2006) *Energy Convers Manag* 47:3185
- You M, Zhang XX, Wang JP, Wang XC (2009) *J Mater Sci* 44:3141. doi:10.1007/s10853-009-3418-7
- Cao Q, Liu PS (2006) *Eur Polym J* 42:2931
- Liu PS, Li YF (1991) *Polym Mater Sci Eng* 7:60
- Anant S, Buddhi D, Sawhney RL (2008) *Renew Energy* 33:2606
- Wang WL, Yang XX, Fang YT, Ding J (2009) *Appl Energy* 86:170
- Wang XW, Lu ER, Lin WX, Liu T, Shi ZS, Tang RS, Wang CZ (2000) *Energy Convers Manag* 41:129
- Cao Q, Liu PS (2007) *J Mater Sci* 42:5661. doi:10.1007/s10853-006-0884-z
- Yan QY, Liang C (2008) *Sol Energy* 82:656
- Okerberg BC, Marand H (2007) *J Mater Sci* 42:4521. doi:10.1007/s10853-006-0471-3